

F. Mocellin, E. Melleras and
W. L. Guesser

Tupy Fundições Ltda
R. Albano Schmidt, 3400
89206-900 Joinville, SC. Brazil
fabianom@tupy.com.br
meller@tupy.com.br
wguesser@tupy.com.br

L. Boehs

Universidade Federal de Sta Catarina
Depto de Eng. Mecânica
Campus Universitário
88040-900 Florianópolis, SC. Brzil
lb@grucon.ufsc.br

Study of the Machinability of Compacted Graphite Iron for Drilling Process

CGI – Compacted Graphite Iron – has reached an important status for automotive industry, mainly in the last ten years. The material has been used for manufacturing parts as brake discs, exhaust manifolds, engine heads and diesel engine blocks. The superior strength characteristics of CGI, as compared to gray iron, allows the manufacturing of engines for higher pressure operating combustion chambers, therefore more efficient and with lower emissions levels. Also thinner walls are possible, generating lighter engines. However there are some technical challenges to overcome, mainly related to the machining process of the parts. This research intends to study the machinability of CGI, in order to develop a new alloy with improved characteristics of machinability, so the production costs for CGI automotive parts can be reduced. The study uses a reference material, gray iron FC-250, widely used for engine blocks manufacturing. The machinability of the referred material is compared to five different CGI alloys by means of drilling experiments. The considered machinability criteria are the tool wear and the cutting forces. The experiments led to the development of a CGI-450 with machinability 83% (relative to FC-250), therefore with excellent potential qualities for engine block and other auto parts manufacturing. **Keywords:** Compacted graphite iron, CGI, drilling, machining, machinability

Introduction

Compacted Graphite Iron has been increasingly accepted as automotive manufacturing material, showing its efficiency for several components, as brake discs and brake drums, exhaust manifolds, engine heads and diesel engine blocks, traditionally manufactured from gray cast iron (Guesser and Guedes, 1977). CGI allows the manufacture of diesel engines with better characteristics of combustion and performance. Due to its good mechanical properties (Guesser et al., 2001), higher pressures are possible in the engine combustion chamber. The main drawback of using CGI for engine blocks is its poor machinability, as compared to gray cast iron, leading to higher production costs. The present research has the purpose of developing new alloys of CGI with improved machinability characteristics, which can also be used for engine heads and other auto parts manufacturing.

This research was conducted as a partnership between the Universidade Federal de Santa Catarina (Federal University of Santa Catarina) and Tupy Fundições Ltda (Tupy Foundry). Tupy has the new technology expertise to obtain the CGI, free of Ti addition.

Nomenclature

$1-m_c$ = Cutting force Kienzle Equation exponent

$1-m_f$ = Feed force Kienzle Equation exponent

b = Chip width, mm

D = Diameter of the drill, mm

f = Feed per revolution, mm

F_c = Cutting force, N

F_f = Feed force, N

h = Chip thickness, mm

T = Torque, N.m

VB_{max} = Maximum tool wear, mm

V_c = Cutting speed, mm/min

$K_{c1.1}$ = Specific cutting force, N/mm²

$K_{f1.1}$ = Specific feed force, N/mm²

Compacted Graphite Iron

The extensive use of gray cast iron for manufacturing engine blocks is related to its excellent machinability, good vibration damping capacity, good thermal conductivity and low production cost. The good thermal conductivity is due to the interconnected graphite flakes, which has higher thermal conductivity than the matrix (Jaszczak, 2001). However, the interconnected flake graphite causes the reduction of mechanical strength, ductility and toughness, due to matrix discontinuities and stress concentration effect (Marquard et al., 1998). For the compacted graphite iron, most of the graphite is interconnected, but in a different geometry (Fig. 1), generating slighter discontinuities and lower stress, due to round edges.

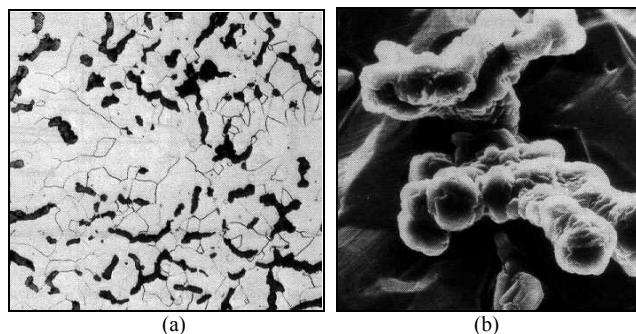


Figure 1. Microstructure of cast graphite iron. (a) Optical Micrograph. (b) 3-D shape of compacted graphite. MEV 395x (ASM, 1996).

The graphite shape is the basic difference between CGI and gray iron. This difference is the main reason for better mechanical properties of the compacted graphite iron, especially mechanical and fatigue strength, and a small loss on thermal conductivity and damping capacity. The properties of gray cast iron, compacted graphite iron and ductile iron are compared on Tab. 1. It can be seen that the values of the properties of compacted graphite iron lie between the gray and the ductile iron ones.

¹Presented at COBEF 2003 – II Brazilian Manufacturing Congress, 18-21 May 2003, Uberlândia, MG. Brazil.

Paper accepted October, 2003. Technical Editor: Alisson Rocha Machado

Table 1. Comparative mechanical and physical properties of different types of cast iron. (The index 100% was assigned to compacted graphite iron for comparison purposes) (SAE J1887/2002).

Property	Gray Iron	CGI	Ductile Iron
Ultimate Tensile Strength	55 %	100 %	155 %
Yield Strength	-	100 %	155 %
Elastic Modulus	75 %	100 %	110 %
Fatigue Strength	55 %	100 %	125 %
Hardness	85 %	100 %	115 %
Damping Capacity	285 %	100 %	65 %
Thermal Conductivity	130 %	100 %	75 %

The CGI manufacturing technique is decisive for its resulting machinability. The change in the graphite shape, from flake to compacted, is due to the action of magnesium, which is a nodulizing element. In order to build up the compacted graphite shape, the amount of magnesium must be kept between 0,010 % and 0,012 %. As this composition control is difficult to maintain for regular casting processes, titanium is used in some cases as anti-nodulizing element, between 0,1 and 0,2 %, which enlarges the possibility of obtaining compacted graphite iron for higher percentages of magnesium. There is a drawback resulting from the Ti addition, caused by the precipitation of titanium carbide and carbonitride hard inclusions, which compromises the machinability of the product (Dawson et al., 1999; Dawson, 1994). This is the reason why Ti is not used for cylinder blocks and heads. At Tupy Fundições, it is used the SinterCast Process to control the Mg amount in a narrow range.

Influence Factors on CGI Machinability

Dawson et al. (1999) classified the important variables related to machinability of compacted graphite iron as follows:

- Graphite shape effects;
- Pearlite effects;
- Chemical elements effects (Sb, Mn, Si, S, Ti, Cr);
- Inclusion effects.

Although each of the listed variables could be extensively discussed, this work proposes to examine only the effects of variables existing in the materials tested.

Graphite Shape Effects

The chip formation for cast iron is directly affected by the presence of graphite, which is known to have low mechanical strength and generate discontinuities and stress concentration effects in the matrix, therefore helping the material removal process. The chip formation mechanism is shown in Fig. 2 for gray iron and ductile iron. At the start, the tool compresses the material underneath the flank creating a fracture, which propagates ahead and beneath the cutting edge (a). As the cutting motion of the tool proceeds, the material fragment is completely detached (b). For some situations, especially with gray iron, a piece of material is tear off ahead of the tool, causing a temporarily lost of contact between tool and workpiece, until the next chip (c). The tear of material contributes for the higher surface roughness of the workpiece (d). For ductile cast iron the permanent strain is larger and the tear of material smaller (Cohen et al., 2000). The chip formation behavior for the compacted graphite iron lies between the ductile and gray behaviors (Reuter et al., 1999).

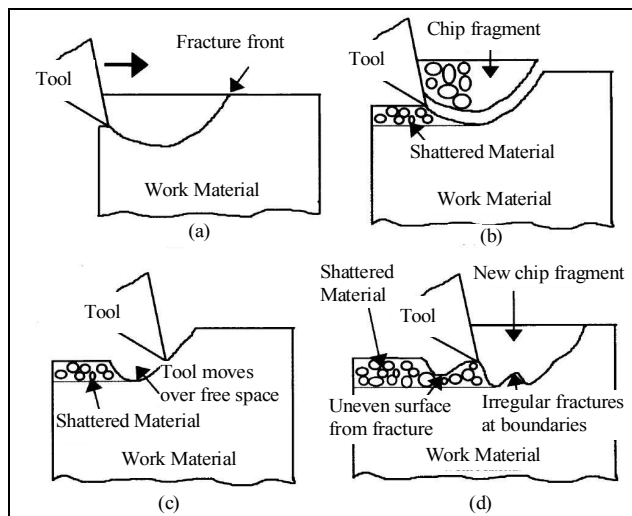


Figure 2. Schematic sequence of chip formation for cast irons (Cohen et al., 2000).

Influence of the Pearlite Content

The mechanical strength of cast irons is proportional to the ratio pearlite/ferrite if the remaining variables are kept constant. However higher pearlite contents is not necessarily the cause of higher tool wear.

Turning tests results, discussed by Dawson et al (1999) were carried out for compacted graphite iron with different values of pearlite contents. Cu and Sn were used as stabilizing elements. In order to reach 100% of pearlite, Mn was also added. The tests used carbide tools, with cutting speeds of 150 and 250 m/min (Fig. 3).

For the pearlite range between 70% and 97,5%, and 150m/min cutting speed, the tool life unexpectedly shows its higher value at 75%. The tool life used for the Mn alloy (100% pearlite) was suddenly reduced. This is not due to the 2,5% increase on pearlite, but to the changes of microhardness of ferrite and other microstructure variations (Dawson et al., 1999).

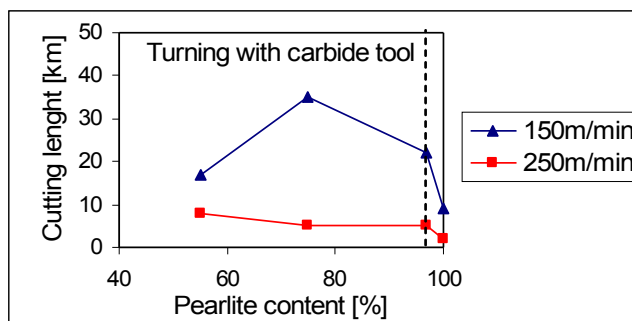


Figure 3. Pearlite contents influence in machining compacted graphite iron (Dawson et al., 1999).

Sulfur Effects

Sulfur, together manganese, forms manganese sulfide (MnS). Boehs (1979) states that the presence of MnS in ferritic blackheart malleable iron improves the machinability mainly because of improvement of chip braking.

Inclusions of MnS usually improve the machinability of gray irons and "free cutting" steels, acting as lubricant. The adherence of MnS to the tool surface creates a lubricating layer, protecting also against oxidation and diffusion, specially at high cutting speeds. For

CGI there is no building of such layer since the regular amount of sulfur lies around 0,01%, i.e., ten times lower than for gray iron. Moreover, the residual sulfur in compacted graphite iron combines with magnesium, nodulizing element, so there are no remaining quantities to combine with manganese and to form the MnS protective layer (Reuter et al., 2000).

Methodology

Characterization of Materials

The studied materials are: gray iron FC-250 and five different types of CGI, manufactured using the SinterCast process, with no added Ti. For this paper, the materials are identified from A to F, according to their specific characteristics, as shown in Table 2. The different properties were attained by controlled changes of casting parameters. The microstructures of Gray Iron A, CGI D and CGI F are shown in Figs. (4), (5) and (6) respectively. In Fig. (4) it is shown the typical graphite of gray iron in a fully pearlitic matrix. In Fig. (5) it can be seen the compacted graphite, and some nodules. The amount of pearlite is almost 100%. The CGI F, shown in Fig. (6), is significantly different from the others, due to its lower amount of pearlite.

Machinability Tests

The drilling tests were performed for cylindrical specimens, with 104 mm diameter and 29 mm thickness. For each specimen, the end face was machined, and from this face 39 holes with 22 mm depth were drilled. The wear of the drill was measured for each machined specimen. The drills used are solid carbide from class K35, diameter 10 mm, TiAlN single layer coated (3.000 HV), geometry by DIN 6537, right cut, long series, Walter brand, code B1422.Z.10,0.Z2.49. A hydraulic mandrill Mapal brand, code 10 sc 0799 was used. The drilling tests were performed by a vertical milling machine CNC, 3 axes, Romi brand, model Polaris F400. The cutting parameters are: $V_c = 80$ m/min $f = 0,25$ mm.

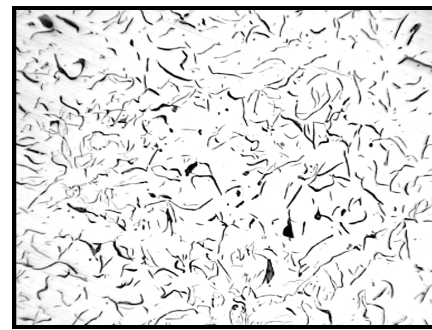
Drill Life Span Criterion

The performance evaluation of drills during tests was based on the maximum flank wear (VB_{max}). Fig. 7 shows the position of VB_{max} , over the diameter. The life span is ruled by a maximum flank wear of 0,40 mm, equals to the drill guide width.

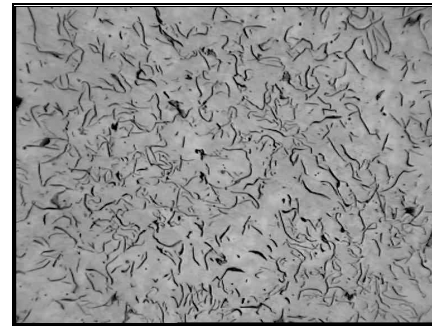
Table 2. Characteristics of studied cast irons.

Properties	Materials					
	Gray A (batch 1 batch2)	CGI B	CGI C	CGI D	CGI E	CGI F
% nodules	Lamellar	36	8	9	14	11
% pearlite	97/100	99	84	89	90	39
Hardness ¹ [HB]	214/223	229	237	229	229	173
Grade	250	550	450	450	450	350

1. Brinell Hardness for 5 mm diameter ball and 7.355 N force.

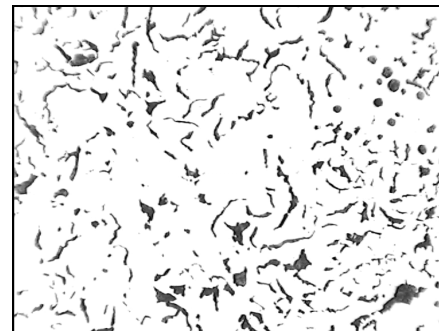


(a)

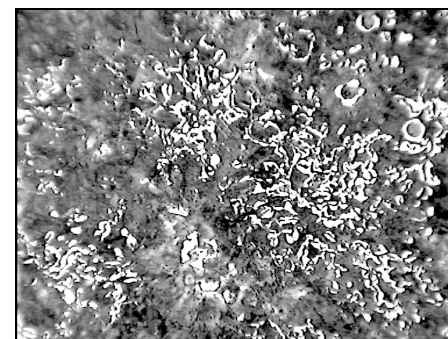


(b)

Figure 4. Microstructure of Gray Iron A completely pearlitic: (a) without etching; (b) with nital etching 2%. (100x magnification).



(a)



(b)

Figure 5. Microstructure of CGI D: (a) without etching; (b) with nital etching 2%. (100x magnification).

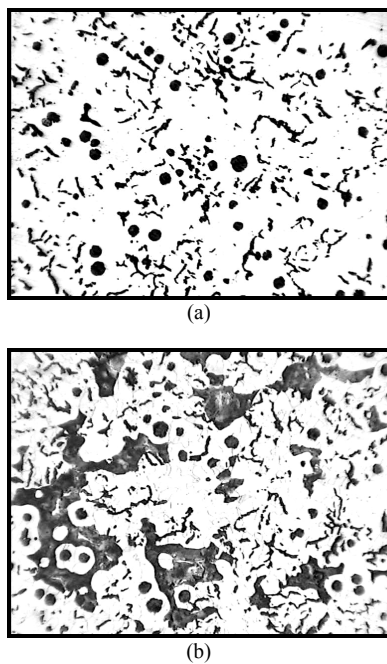


Figure 6. Microstructure of CGI F: (a) without etching; (b) with nital etching 2%. (100x magnification).

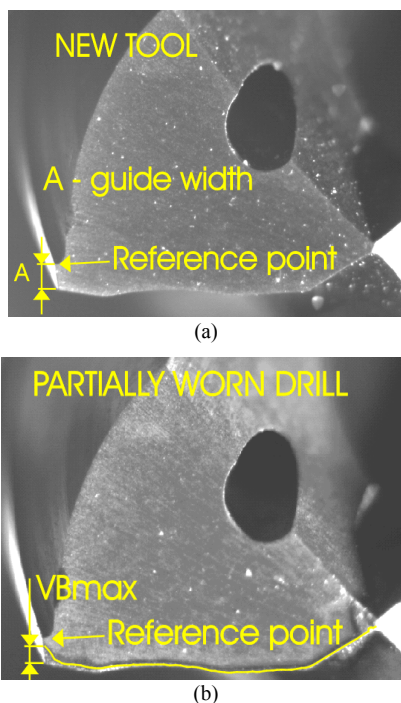


Figure 7. (a) Drill showing no wear; (b) drill with flank wear.

Cutting Force Measurements

Cutting and feed forces measurements were taken with a piezoelectric platform, Kistler Instrumente 9273, with error less than 1% for the testing range of loads. The used parameters for evaluating forces were: $V_c = 80$ m/min e $f = 0,20$ mm. For the specific cutting and feed forces determination ($K_{c1,1}$ and $K_{f1,1}$), were used the feeds 0,10, 0,20 e 0,25 mm.

Results

The studied materials were manufactured under different chosen casting parameters, in order to evaluate materials with different machinability grades.

Machinability of Gray Iron a compared to CGI B

Those tests were essentially aimed to the comparison of the material presently used for engine blocks, cast iron FC-250, with the compacted graphite iron class CGI-550. Both materials are almost completely pearlitic.

The machining tests of the above mentioned materials have shown significant differences in the tools life span (Fig. 8). The Gray Iron A curve show less tool wear at the beginning of the test, sustaining this behavior for all machined length. The drills used for CGI B have shown an average life span around 44% of the corresponding value for Gray Iron A (Fig. 9). This result is similar to that reported by Reuter (2000), which in 1995/1996 machined several CGI engine blocks in transfer lines. Reuter justified this difference based on the higher mechanical strength of compacted graphite iron, which is approximately twice the corresponding value for gray iron. Dawson et al. (1999) state that the addition of some elements to form a fully pearlitic matrix may alter ferrite and cementite composition and hardness of the pearlite, causing a loss of machinability.

The CGI B has a high amount of nodular graphite (36%), which is beneficial to mechanical properties. However there is a negative effect on the machinability, since a closer contact between tool and workpiece is promoted.

Machinability of CGI-450 Materials (C, D and E)

These materials are classified as CGI-450. The CGI C, which has the higher hardness among the studied materials, has shown 67% machinability, compared to reference – Gray Iron A. The wear behavior of the tool is shown in Fig. 10. The CGI D has 5% more pearlite and lower hardness than the CGI C. Although CGI C and D belongs to the same class of mechanical strength, CGI D was produced under controlled casting parameters, leading to a 25% machinability gain, as compared to CGI C, reaching 83% of the reference value (Fig. 9). This is an encouraging result, considering that a material with recognized poor machinability, achieved tool wear behavior close to the gray iron.

The CGI E has a larger amount of pearlite former elements when compared to CGI D, and 5% more nodular graphite. Both have the same pearlite contents and hardness. Their similarities were confirmed during the machining tests (Fig. 10). The tool used for CGI E – which has higher amount of pearlite former elements – had a smaller span life, 78% compared to Gray Iron A. By its turn, CGI D reached 83% for life span. The statistical tests applied to tool wear, considering a 95% confidence level, indicate that the difference between D and E is not statistically significant. Among all tested materials CGI D and E are the only ones that did not show significant behavior differences.

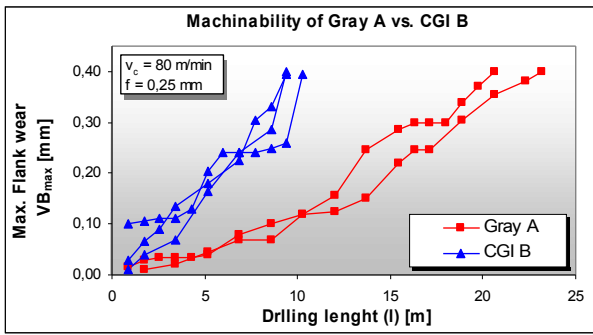


Figure 8. Wear curves for Gray Iron A (FC-250) and CGI B (CGI-550).

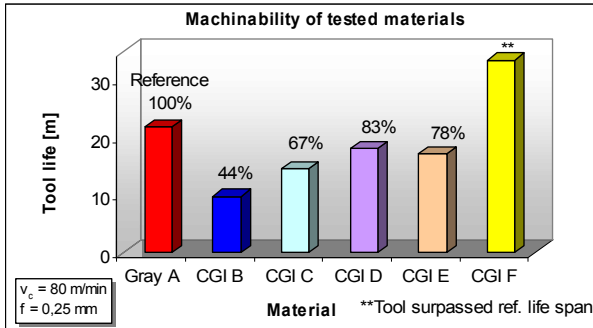


Figure 9. Comparison of machinability of tested materials, using $VB_{max} = 0,40$ mm criterion.

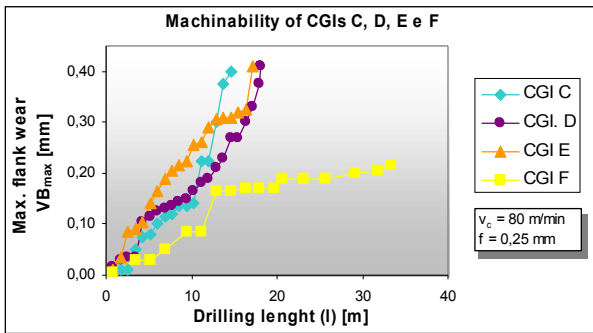


Figure 10. Wear behavior of drilling tools with CGI, types C, D, E e F.

Machinability of CGI-350 (F)

This particular result makes evident the influence of the pearlite forming elements, and by consequence, the pearlite content. The machinability of CGI F, with 39% pearlite, is much higher than for Gray Iron A (Fig. 9). The wear behavior curve (Fig.10) shows a tool wear around 0,20 mm, at 33 m drilling length when test was interrupted. This value of VB_{max} is only half the life span criterion.

It must be emphasized that, in spite of its excellent machinability, CGI F has low hardness, low mechanical strength, and low pearlite. These factors are a drawback for its use in engine blocks, however it can be employed for other parts such as engine heads.

Cutting Forces Measurements Results

Three holes were machined for the torque evaluation, and three for the feed force evaluation, for each of the studied materials. The results are shown in Fig. 11.

The measurements were statistically analyzed for significance, with 95% confidence level. For the torque evaluation the scattering of values does not allow to conclude that there are significant differences between the studied materials, for the number of taken measurements. For the feed forces, it was concluded that only the CGIs D and E do not have significant differences. The feed force machinability criterion has shown coherence with the VB_{max} machinability criterion for all tested materials.

Determination of Kienzle Equation Constant and Exponent

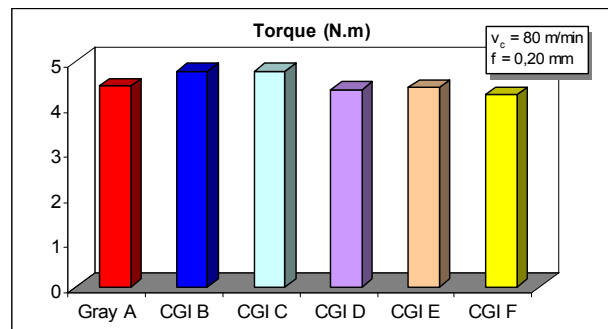
From Kienzle Equation and its constants, the cutting and feed drilling forces can be calculated for different chip widths (b) and chip thickness (h). The Kienzle Equation constants are machinability parameters of the material itself, then conceptually independent of the machining process. Nevertheless, the drilling constants cannot be used for other processes, because the equation does not consider variables as tool geometry, tool material, tool type and process type.

The Kienzle Equation constants (Eq. 1) were empirically determined for: Gray Iron A and CGI C. The twisting moment values were converted to forces using Eq. (2).

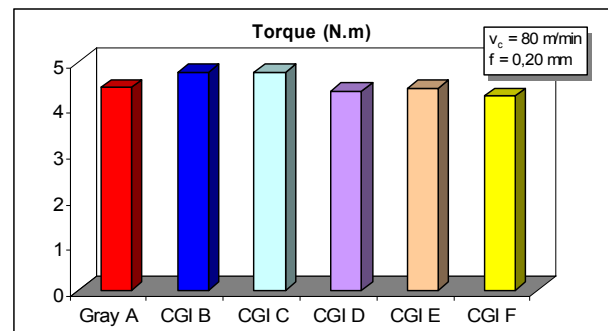
$$F_c = k_{c1.1} \cdot b \cdot h^{1-m_c} \quad \text{and} \quad F_f = k_{f1.1} \cdot b \cdot h^{1-m_f} \quad (1)$$

$$F_c = \frac{T}{0,38 \cdot D} \quad (2)$$

The measured values of specific cutting force ($K_{c1.1}$) and the exponent of the Kienzle equation ($1-m_c$) are shown in Fig. (12.a). The specific feed force ($K_{f1.1}$) and the corresponding exponent ($1-m_f$) are shown in Fig. (12.b). CGI C has 7% higher cutting force and 29% higher feed force than Gray Iron A. The coefficients ($1-m_c$) and ($1-m_f$) show very small difference for the two materials.

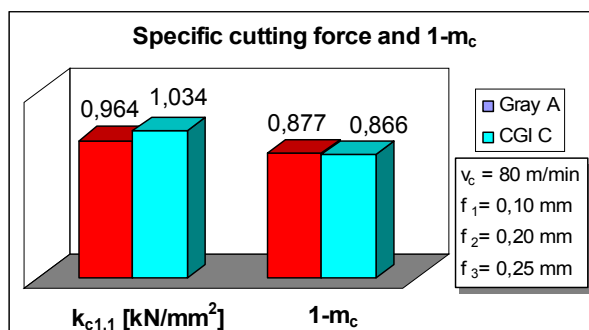


(a)

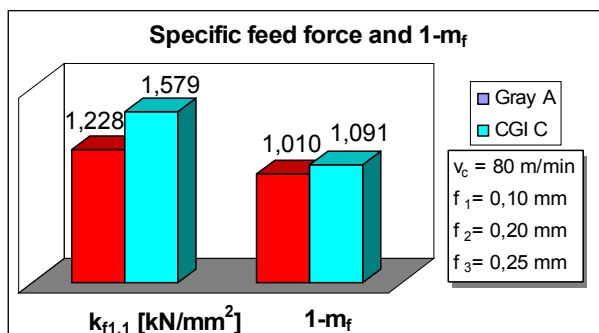


(b)

Figure 11. Torque measurements (a); feed forces measurements (b).



(a)



(b)

Figure 12. Empirically determined Kienzle Constants, for cutting force (F_c) and feed force (F_f) calculations.

Conclusion

The obtained results generate good expectations for the use of compacted graphite iron. The following comments are valid for drilling, and may be not applicable to other machining processes.

The controlled casting parameters made feasible to obtain CGIs with a large range of machinability.

The alloying elements, added to build 100% pearlite, generated a CGI class 550 (CGI B) with only 44% machinability compared to reference material – Gray Iron FC-250.

When high amounts of pearlite and high hardness are not required, as in the case of engine heads, the CGI Grade 350 is recommended. Its mechanical strength is lower than CGI 450 but has much higher machinability, due to its low pearlite contents.

The class 450 compacted graphite irons have machinability values between 67% (CGI C) and 83% (CGI D). Among the tested materials, the most appropriate for manufacturing engine blocks is CGI D. It combines a machinability only 17% below Gray Iron FC-250, high pearlite contents, high mechanical strength and hardness.

Acknowledgements

The authors acknowledge CAPES and Tupy Fundições Ltda for their financial support.

References

ASM. Speciality handbook: cast irons. United States: ASM International, 1996, p. 33-267.

Boehs, Lourival. Influência do sulfeto de manganês na usinabilidade do ferro fundido maleável preto ferrítico. 1979. 105 f. Dissertation (Mechanical Engineering Master Degree) – Departamento de Engenharia Mecânica, Universidade Federal de Santa Catarina, Florianópolis.

Cohen, P. H.; Voigt, R. C. and Marwanga, R. O. Influence of graphite morphology and matrix structure on chip formation during machining of ductile irons. In: AFS Casting Congress, American Foundrymen's Society, Pittsburg, 2000.

Dawson, Steve et al. The effect of metallurgical variables on the machinability of compacted graphite iron. In: Design and Machining Workshop – CGI, 1999.

Dawson, Steve. The SinterCast Process and compacted graphite iron. In: International Conference on Latest and Best in Melting and Metal Treatment in Ferrous and Non-Ferrous Foundries, Coventry, England, 1994.

Guesser, L. W. and Guedes, L. C. Desenvolvimentos recentes em ferros fundidos aplicados à indústria automobilística. In: IX Simpósio de Engenharia Automotiva, AEA, São Paulo, 1997.

Guesser, W; Schroeder, T. and Dawson, S. Production Experience with compacted graphite iron automotive components. AFS Transactions, Des plaines, 2001.

Marquard, Ralf; Helfried, Sorger and McDonald, Malcolm. Crank it up: New materials create new possibilities. Engine technology international, v. 2, p. 58-60, 1998.

Jaszczak, John A. Michigan Technological University, Department of Physics at the A. E. Seaman Mineral Museum. The graphite page. Available at: <<http://www.phy.mtu.edu/faculty/info/jaszczak/graphite.html>>. Access dec. 17, 2001.

Reuter, Ulrich, et al. The wear process of CGI cutting and machining developments. In: Compacted Graphite Iron – Machining Workshop, Darmstadt, Germany, 2000.

Reuter, Ulrich, et al. Wear mechanisms in high-speed machining of compacted graphite iron. In: Design e Machining Workshop – CGI, 1999.